International Journal on Advanced Science Engineering Information Technology

Vol.12 (2022) No. 2
ISSN: 2088-5334

Increase in Torque and Power of an Otto 200cc Spark Ignition Engine with Modifications in the Combustion Chamber

Vicente Rojas-Reinoso [a,*], Johnny Pancha-Ramos [b], Vicente Romero-Hidalgo [c], Jorge Martinez-Coral [d], Ivan Zambrano-Orejuela [d]

[a] *Carrera Ingeniería Automotriz, Universidad Politécnica Salesiana, Rumichaca y Morán Valverde, Quito, 170606, Ecuador*
[b] *Facultad de Mecánica, Escuela Superior Politécnica de Chimborazo, Panamerica Sur, Riobamba, 060106, Ecuador*
[c] *Ingeniería & Arquitectura, Universidad de Castila La Mancha , C/ Altagracia 50,Toledo, 45071, Spain*
[d] *Facultad Mecánica, Escuela Politécnica Nacional , Ladrón de Guevara E11·253,Quito, 170525, Ecuador*

Corresponding author: [*]erojas@ups.edu.ec

***Abstract*— Study of the behavior of a single-cylinder type spark ignition Otto engine with a cylinder capacity of 200 cubic centimeters, which generates a modification in the geometry of the combustion chamber to increase the compression ratio, reaching optimal operating conditions; in order to optimize torque, power, polluting emissions and something fundamental in the social reality of Ecuador, fuel consumption. Variables are determined to be applied in a generic experimental model under controlled conditions with the application of an analysis protocol based on the use of a probe in conjunction with a piezoelectric sensor for various tests based on the effective mean pressure in different engine load cycles, using an electronic acquisition card controlled with LabVIEW software. In the testing cycle, several conditions are considered as the instantaneous speed of the vehicle with attention to the INEN 960 standard, achieving results of an increase in power of 5.85 kW, torque at 0.78 N.m, decrease in CO emissions by 13%, and HC 6.47%, and with a reduction in fuel consumption of 3.35% compared to initial conditions. These results indicate the importance of the study of effective mean pressure as a parameter of a validated experimentation model. The study projections in the branch of analysis of the indicated and real effective mean pressure allow to generate a better control in the combustion process, showing a real stability model according to the engine's behavior characteristics and work requirements.**

***Keywords*— Torque; power; tractor force; DAQ; average pressure; emissions.**

Manuscript received 21 Apr. 2021; revised 11 Sep. 2021; accepted 18 Nov. 2021. Date of publication 30 Apr. 2022.

I. INTRODUCTION

The increase in the consumption of fossil fuels increases considerably as industrialization and energy demand in the world increase, forcing countries to look for energy alternatives sources. Akal *et al.* [1] indicate that to reduce demand or, above all, improvement of engine performance or other vehicle systems should work directly with fuel efficiency and performance and polluting emissions. It is also to generate the deepening of dual fuels engines to control engine emissions equally, as indicated by Ramazan *et al*. [2]. Four-stroke injection systems, the power stroke, are the most important stroke to make combustion operation. The main factor that affects the engine's performance is how the combustion process behaves, generating an increase in pollutant emissions associated with the conversion of chemical energy from the fuel into thermal energy [3].

The mean pressure is determined as a constant value resulting from the average that an amount of power will produce by different fuels that can be used, which has been generated that at a motor speed, a great load produces and good efficiency results [4]. However, it should not decrease because it reflects less power generation; this average value resulting from the pressures generated inside the cylinder at the time of the explosion is considered a condition similar to the effective work of an internal combustion engine [5].

The variation of the pressure in the cylinder can be interpreted utilizing the work cycle of an internal combustion engine. It is a variation and different behavior of the pressure inside the cylinder as the crankshaft goes through the degrees of rotation in the whole operation to present an increase and characteristic interaction of the pressure inside the cylinder when they are at the moment of ignition and expansion as shown in Figure 1 [6].

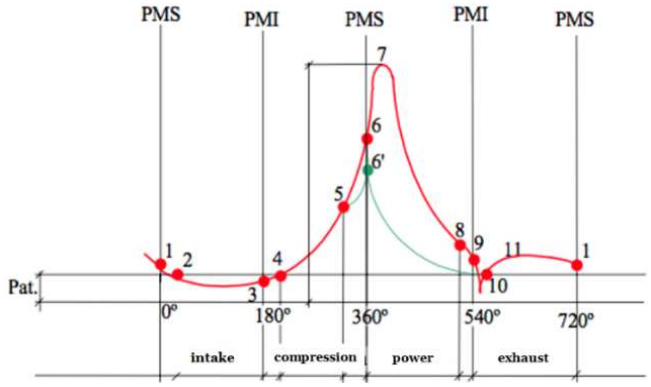

Fig. 1 Pressure diagram in relation to crankshaft time [5]

The pressure that presents variations during internal combustion engine operation can be interpreted by applying a pressure sensor that has been installed inside the cylinder, capable of detecting the different pressure variations during the engine's cycle concerning the revolutions per minute (m^{-1}). The sensor's processing of these electrical signals is subject to reducing all electrical noise in the signal employing a zero-pass filter with the obtaining of fundamental signals from the motor such as the airflow at the intake, intake manifold absolute pressure, and internal combustion engine load. Figure 2 shows the signal generated by the sensor before and after being processed [7].

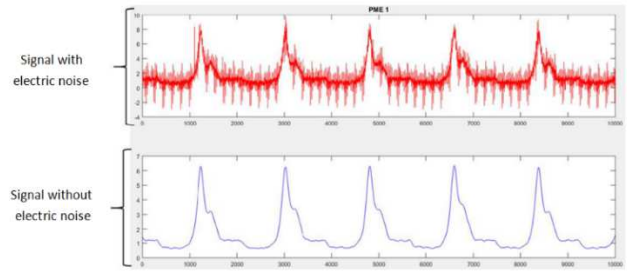

Fig. 2 Signal from the pressure sensor inside the cylinder [7]

Detecting each behavior of the generated signal allows knowing the operating cycle of the piston in the cylinder. The incidence that the different interactions of the signal have to be used to model the torque and power of the internal combustion engine [8]. Figure 3 shows the work cycles from point 1 to 2 the admission time, from point 2 to 3 the compression time is observed, from point 4 to 5 the expansion time, and finally from point 5 to 6 the show escape time [9].

It is important to filter this electrical signal to achieve a better curve of the effective mean pressure, and this is the most real without electrical noise or parasitic currents, which allows adapting a better pressure behavior in the graphs and study results. For Castresana *et al.* [10], implement a Butterworth filter to filter the largest signals generated in operation and determine that the filter considers a cut off frequency at a value of 0.05 Hz, relating the path from the top dead center in such a way as to achieve the curves for the analysis of the graphs and they are real continuously with the travel of the crankshaft [11].

This method of obtaining the effective mean pressure is used in other studies that obtain torque and power, according to Fang [12]. This method calculates the mean effective pressure of the fuel/air mixture. In the piston head the force is generated, which is transmitted to the connecting rod and the interaction of the inertial forces [13]. Said inertial forces are obtained as a function of the crankshaft rotation, be it the measured angle of the crankshaft and the motor's rotation speed, which allows simultaneously to acquire the pressure in the cylinder and also thrust force on connecting rod [14].

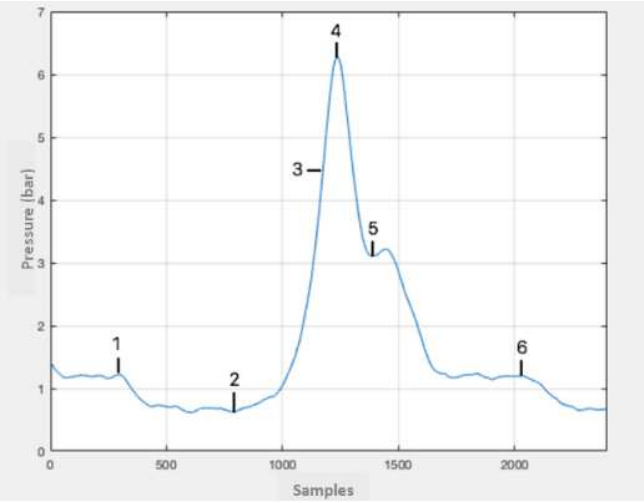

Fig. 3 Cycle of the signal from the pressure sensor inside the cylinder [7]

In Figure 4, details the forces that act on the piston and the piston rod at the moment when the crankshaft rotates in ignition conditions, the effect of the power inside the combustion chamber that produces energy to be able to have the reciprocating movement piston, where piston-assembly friction (Ff) can be obtained from the force of the compression (Fc), rod force (Fstg), gravity (mpg) and finally the inertial forces (Fin,Fcin). According to Chengwei *et al.* [15], the joint piston-connecting rod work is generated by the force of the combustion of the mixture, the push of the connecting rod, gravity, which additionally with the inertial forces based on the instantaneous balance of forces.

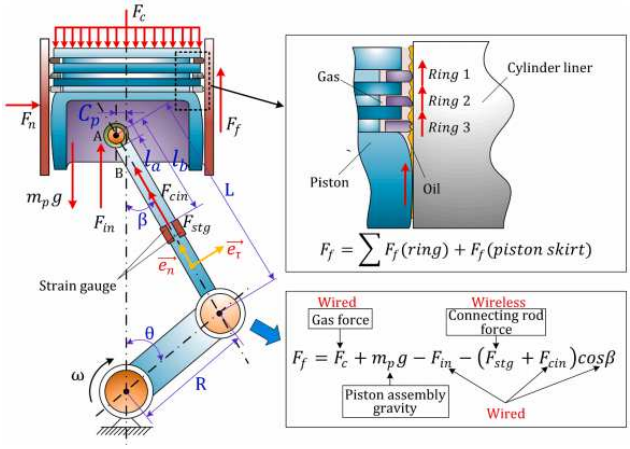

Fig. 4 pressure sensor inside the cylinder [15]

Motorcycle engines operate in incomplete combustion, with very poor emission control and aftertreatment technologies, generating more pollutant emissions per mileage than automobiles. Motorcycles are forced to update their emission standards, first improving the fuel/air mixture preparation system [16].

It is still far from satisfying. Therefore, to improve the emission situation and environmental impact factors, it is necessary to estimate the number of emissions and the operating condition of the motorcycle engines in an entire driving cycle., as shown in [17].

Vehicle emission standards are the primary technical policy tools available to mitigate vehicle emissions. Emissions test procedures for light vehicles are based on a transition cycle that represents the driving pattern of a particular country. Cycles for light service vehicles are FTP-75 and NEDC used in the United States and European testing procedures, respectively. Emission factors are the average number of pollutants emitted by a vehicle type [18]. These are said in terms of pollutant mass emitted per unit distance traveled or per unit of fuel consumed. Determining these factors poses major challenges for environmental authorities [19]. Figure 5 shows the representation of the FTP-75, the cycle that the EPA uses expressed in miles per hour and seconds for the standardization of consumption and emissions.

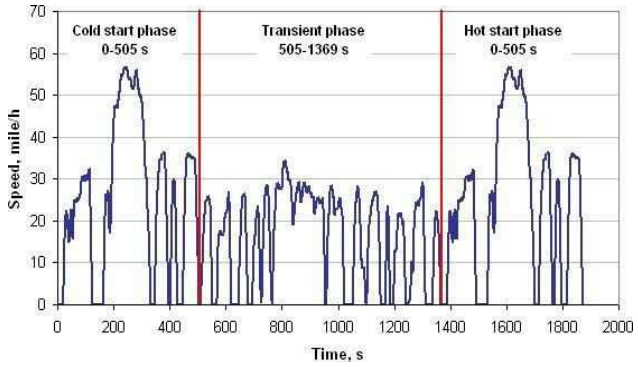

Fig. 5 FTP-75 cycle used by the EPA to certify emissions [19]

Estimating consumption in motorcycles follows the WMTC (Motorcycle Cycle World Test) procedure, which considers different road conditions, be they urban, suburban, or highway, considering the driving mode. The WMTC procedure is characterized by frequent braking, strong acceleration, and reaching the limit speeds of each type of road, considering its very representative results in terms of the actual consumption of a motorcycle in daily use. Figure 6 shows ECE R47 test cycle used for Euro 2 and Euro 3, as for the Euro 5 use WMTC.

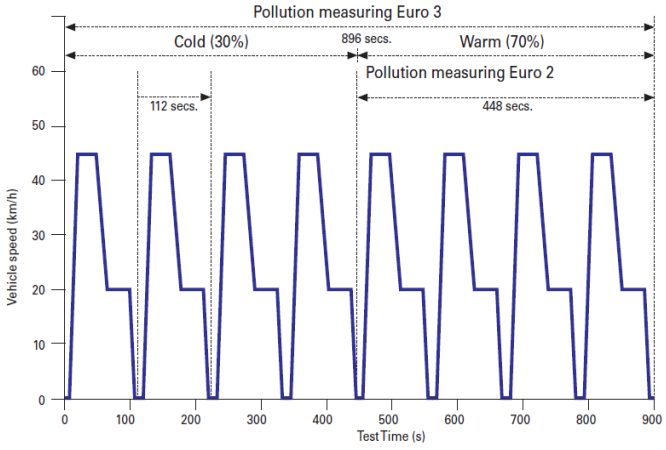

Fig. 6 ECE R47 test cycle

It is essential to emphasize that the tests are carried out on a motorcycle with standard characteristics. It must be estimated that the consumption data provided by the manufacturers are always far from the real ones, which will depend on different unpredictable factors that can increase fuel consumption [19]. Table 1 shows the environmental requirement for motorcycle for Euro 2, Euro 3, and Euro 5 [20].

TABLE I
ENVIRONMENTAL REQUIREMENT FOR MOTORCYCLES

Euro 2 and euro 3 step						
Category	Vehicle Category	Classification [cm^3]	Euro	Mass of [mg/km]		
				CO	THC	NOx
				L_1	L_2	L_3
L3e	two-wheel motorcycle	<150	2	5.500	1.200	300
		≥150	2	5.500	1.000	300
		<150	3	2.000	800	150
		≥150	3	2.000	300	150
		<130 km/h	3	2.620	750	170
		≥130 km/h	3	2.620	330	220
Euro 4 step						
L3e	two-wheel motorcycle	PI/CI/Hybrid V_{max}<130 km/h	4	1.140	380	70
L4e	With and without side car		4	1.140	170	90

As with the number of injections, they can obtain a higher effective mean pressure, as mentioned by Yang *et al.* [21]. Acquiring data to measure the pressure in the cylinder in real-time is an alternative for several sensors today. It can reduce calibration costs by providing diverse, accurate information and less than 7% [22]. However, piezoelectric sensors can be used; although they are very expensive, the measurement variation due to sensitivity is high [23]. The ionic current measurement is a more economical alternative, providing good sensitivity, which will be used in the combustion study process [24].

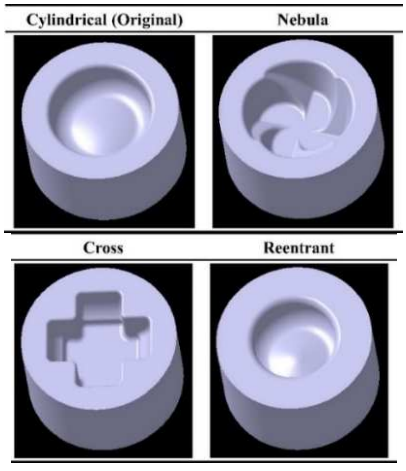

Fig. 7 Combustion Chamber Geometry Design [25]

The use of different fuels in addition to conventional ones also influences the continuous improvement of torque and power. However, it is essential to control and decrease the emissions and improve fuel consumption performance, as indicated by Yangaz [2] and Yan [25]. In addition, Yan [25] revealed that geometric modification is fundamental to

combustion behavior and improvement of MEP (mean effective pressure), as shown in Figure 7.

Alrbai *et al*. [26] consider that the pressure of the engine cylinder depends directly on the piston movement and introduces a new and novel procedure of a model in which it combines algorithms, one for the dynamics converter and the other the cycle in the cylinders, including the combustion process by kinetic chemistry [27]. The algorithms are solved by matrix models in MATLAB®, which are used to predict the working pressure in the engine cylinder.

Another form of study is based on analyzing the acquisition of pressure data inside the cylinder. According to Iscan *et al.* [28], the heat release rate is obtained by filtering and generating the calculation of the algorithm presented to determine the average temperature of the gas, the amount of exhaust gases, and the heat transfer rate. Arsie *et al.* [29] state that the air-fuel mixing factor can estimate the pressure signal in the cylinder. Also, the mass of fresh gases reached in the cylinder can achieve a high precision method through software analysis, which is appropriate to the engine's behavior. Therefore, Rojas *et al.* [30], [31] used the measurement of the cylinder MEP to determine torque and power. Considering the application of a pressure sensor in the cylinder, Gaoa *et al.* [21] determine that it is valid for laboratory studies considering that they are commonly used and have a fairly wide margin of response in terms of application in studies. This is true in the application in the different studies [32]. The study developed by Tadros *et al.* [33] defined that the implantation and placement of these sensors allows obtaining the data for the control algorithm and reviewing the engine optimization. It also develops a cylinder pressure diagram according to the engine behavior data from the cylinder. It works together with the application and obtains different signals to more of those generated by the pressure sensor in the cylinder. It can obtain the crankshaft angle signals depending on the rotation and defines it according to each angle for obtaining pressure diagrams for the different loads applied to the engine in the different tests performed by Skrzek *et al.* [34].

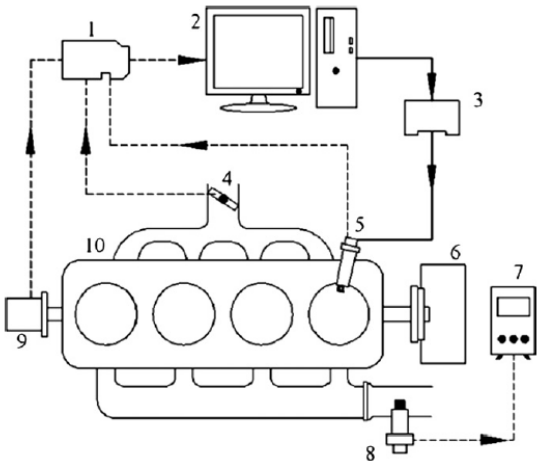

Fig. 8 of the test system. 1-acquisition card, 2-computer, 3-Engine Control Unit, 4 accelerator position sensor, 5 piezoelectric glass sensor, foucault current. 6 dynamometer, 7 lambda analyzer, wide range, 8 oxygen sensor, 9 optical encoder instrument, 10 motor 22.

Zhang *et al*. [35] revealed that with a gasoline engine, variables were considered with the management of sensors. It is under conditions in fuel supply, engine temperature, engine intake, exhaust conditions, and engine revolutions. The cylinder pressure data were acquired by a Kistler 6117BFD piezoelectric glass sensor. The signal is processed and amplified by an acquisition card to obtain cyclic combustion differentiations. However, it is under other operating conditions and effects on engine operating parameters concerning cylinder pressure (5). Figure 8 shows the scheme used for electronic signal collection and management.

In the pressure study, simulating those results allows a comparison of the calculated flame front, using the thermodynamic model with these experimental results achieving a comparison between the different results [36]. Figure 9 details the application of the data obtained to establish an experimental model [37].

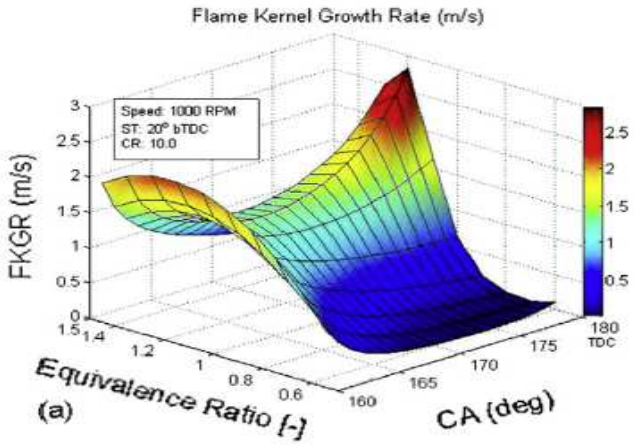

Fig. 9 Application of the data obtained to establish an experimental model

While Salvi *et al.* [38] show the comparison of experimental results of the literature working for the radius of the nucleus of the flame front, as in Figure 10. The simulation results of the presented model show agreement of sane with the experimental results, which allows determining that the application of modeling for validation and obtaining results concerning experimental valuations is possible to perform.

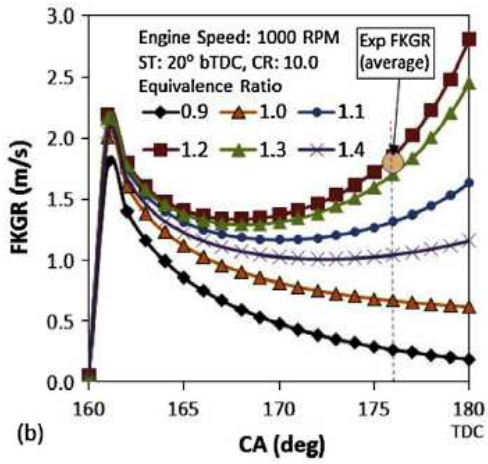

Fig. 10 Compared experimental results of the literature according to the radius of the nucleus of the front of a flame

II. Materials and Methods

The results obtained on torque, power, polluting emissions, and fuel consumption are analyzed in the behavior curves by the conception of a mathematical model and statistical analysis in modifying the geometry of a combustion chamber. Table 2 shows the technical data of the motor used in this study.

A. Torque

To execute the combustion of the air-fuel mixture internally of an engine ignition caused, it is by operation of the ignition spark, which causes an elevation of temperature and pressure to the inside of the engine cylinder. This internal pressure, in turn, produces a power indicated on the piston that displaces it generating the well-known crank-crank mechanism of the alternative internal combustion engines, where the linear movement of the piston becomes a rotating movement of the crankshaft to achieve effective power

TABLE II
RANGER 200CC ENGINE TECHNICAL DATA

Technical engine data	
Year	2015
Cubic capacity	197.4
Work cycles	4Q
Spark plug light clearance (cm^3)	0.8-0.9
Idling (min-1)	900
Prepayment Grades (APMS)	10oG
Intake Valves (Hot) (mm)	0.35
Exhaust Valves (hot) (mm)	0.35
Compression ratio	7.3:1
Total volume cm^3	197.4
Average Pressure (Bars)	2.685
Power Indicated max. (KW)	10.4398
Effective Power (KW)	9.603
Torque (Nm)	10.2

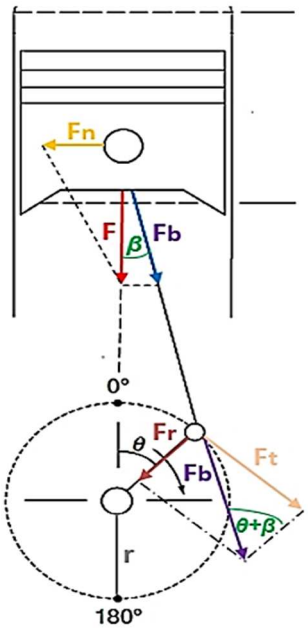

Fig. 11 Scheme for obtaining torque

The force generated by combustion acts on the plunger and is proportional to the characteristic effective mean pressure of an engine that is generated in the expansion stroke [31], being directly proportional to the degree of filling inside the cylinders, compression ratio, displacement of the engine and the energy generated during combustion. In Figure 11, the force executed on the piston is broken down into the force acting on the crank head and in which causes a lateral thrust on the cylinder walls'.FF_b F_n.

Consequently, the product of force by the crank radius establishes the torque, expressed arithmetically in Ec. (1). F_b r.

$$T = F_b * r \tag{1}$$

T: Torque (N.m)
F_b: Force on the crank (N)
r: Crank radius (m)

The force that causes the torque to become variable, which is a 4-course engine is the limit value at the time the combustion time is carried out and then the working time inside the cylinder, being negative the torque in the other times of the engine. When the job is created, and the engine performance is not similar at some points, it depends on the engine's revolutions generating the thrust force that is formed. In this way, the engine's revolutions per minute limit the correct filling of the cylinders and, consequently, the torque. While at low revolutions per minute, the combustion of the mixture does not produce an optimal condition due to the insufficient inertia that the gases have that induces that the filling of the cylinder is not correct, as in the emptying condition. On the other hand, if the engine is kept running at a much higher speed, filling inside the cylinder is not achieved. Due to the limited time, the gas requires to occupy the space available inside the Fcylinder [39]. Yes, achieving an optimal rev time per minute of the engine. However, combustion with more fuel quantity is achieved, and the power is increased further, the torque is reduced. This ensures that specific consumptions are recommended and close to conditions in the maximum torque area in the engine, extending the engine's fuel consumption according to this established condition [40].

B. Power

Power knowledge states how many times the torque is usable, i.e., how fast it can be positioned from the torque. The power developed by an engine is directly proportional to the compression ratio and displacement; at higher values, it is concerned with a greater explosion achieving a higher force applied to the piston; it also depends intimately on the revolutions per minute at which the engine rotates. As a result, the power can be determined by eq. (2).

$$P = T * w = \frac{T*n}{\frac{60}{2\pi}} \tag{2}$$

P : Engine power (kW)
T : Torque or torque (N.m)
w : Angular speed of crankshaft shaft (rad/s)
n : Revolutions per minute (min-1)

After achieving maximum power, the excess revolutions per minute causes reduction. It is due to the fuel injection system reaching an operating limit, unpointed, and it does not achieve enough accuracy to inject the fuel effectively. In

addition, the distribution system is not able to open and close the valves at sufficient speed for exhaust and intake gases to flow properly. The maximum rev limit at which the engine can rotate is set by the limitations of the mechanical elements that constitute it.

C. Relationship between Power and Atmospheric Conditions

Factors that are due to the level of work and atmospheric conditions are temperature, pressure, and conditions of the degree of humidity in the air; all modification parameters have shown a significant impact on the performance and operation of the motorcycle engine. Studies and experience carried out in different aviation engines within chambers in which it is possible to vary the pressure and temperature of the air have shown that the power and torque are proportional to the barometric pressure and inversely proportional to the square root of the absolute temperature. To obtain the same results, the calculation for which the power data obtained in the different test engines whose temperature and pressure conditions have referred to an atmospheric base pressure (760 mm hg) and an ambient temperature (15°C) [34] must be comparable.

$$N_O = N \frac{P_0}{P} \sqrt{\frac{T}{T_0}} \quad (3)$$

No= Air-reduced CV power type
N = CV power gained from the brake
P = pressure atmospheric Kg/cm^2
Po = normal pressure of 760 mm in Kg/cm^2
T = Absolute ambient temperature in °k
To= Normal absolute temperature= (273+15 in °k)

The expression is called the height correction factor regarding humidity. Correction can be made by subtracting the pressure of the verified water vapor from atmospheric pressure and using the resulting value instead of the p-value in the correction $\frac{p_o}{p}\sqrt{\frac{T}{T_0}}$ z. [39]. Replacing the data based on the table results in the following data. Table II shows the calculation value.

TABLE III
CALCULATION VALUES CORRECTION FACTOR AT 2800 METERS ABOVE SEA LEVEL

Altitude (m)	0	2800
Temperature (°K)	288	269,8
Pressure (bar)	1.013	0.710
Air Density (kg/m^3)	1.225	0.928

height correction factor = 1.013/0.710√ (269.8/288)
height correction factor = 1.381

The height value correction formula for passing them at sea level uses the following formula based on the same principle of air density.

$$sea\ level\ correction\ factor = 1 - \frac{1}{height\ correction\ factor} \quad (4)$$

By replacing the results obtained as follows:
sea level correction factor=1- 1/1,381
sea level correction factor= 0,2758
sea level correction factor=28 %

D. Calculations of Cubic Capacity

$$Vh = \frac{D^2 * \pi * S}{4} \quad (5)$$

Where:
D-Diameter
Yes, career
Vh-cylinder volume

$$Vh = \frac{D^2 * \pi * S}{4} \quad (6)$$

$$Vh = 196.4cm^3$$

To develop the proposed analysis, the researchers calculated the compression pressure of the motor (P), the diameter of the piston, the rotation speed of the motor (W) in min-1 and the relationship between the radius of the crank and the length of the crank. Where the following terms are obtained:

L The length of the crank
R Crankshaft turning radius
α Crankshaft position angle
β Crank Angle
P. 170 PSI x 11.95Kg/cm2
Piston diameter 72,967 mm x 7.2967cm
W-3600 min-1 - 471.23 rad/seg
λ= = R/L 34.97/120
0.29 m

Mechanical loss percentage:

$$\%\ \text{Mechanical Lossrdida} = \left(1 - \frac{51{,}45}{56}\right) * 100\% \quad (7)$$

% Loss mechanical = 8.125 %

E. Signal Processing

The pressure sensor used is a BOSCH 0261545053 [41], as shown in Figure 12, with a measurement scale from -5 MPa to 14MPa, with thin-film strain gauge elements poly-silicon metal. These are connected, forming a Wheatstone bridge (an electrical circuit used to measure unknown resistors by balancing the bridge arms). These consist of four resistors that form a closed circuit (the resistance under measurement), with a central signal line and temperature compensation for the measuring range of 48°C with measurement effectiveness of 99.2%. When using work and evaluation of IC, the measurement signal is amplified, correcting it for piston displacement and sensor sensitivity. The functionality features are:

- Evaluation of the radiometric signal (relative to the supply voltage).
- Deviation and sensitivity of self-control.
- Excellent media resistance as the medium only meets stainless steel.
- Resistant to brake fluids, mineral oils, fuel, water, and air.
- Protection against polarity reversal, overvoltage and short-circuit output to supply or ground voltage.

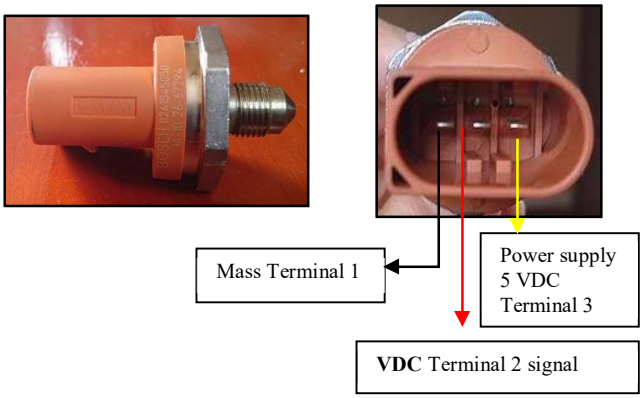

Fig. 12 Polysilicon pressure sensor with range -5MPa to 14 MPa

The scheme used is similar to Zhang [37]; Figure 13 shows the diagram for data capture is direct to the ECU of the sensor capture system, and the calculations are determined according to the characteristics of the vehicle and the torque and power calculations according to the engine design geometry.

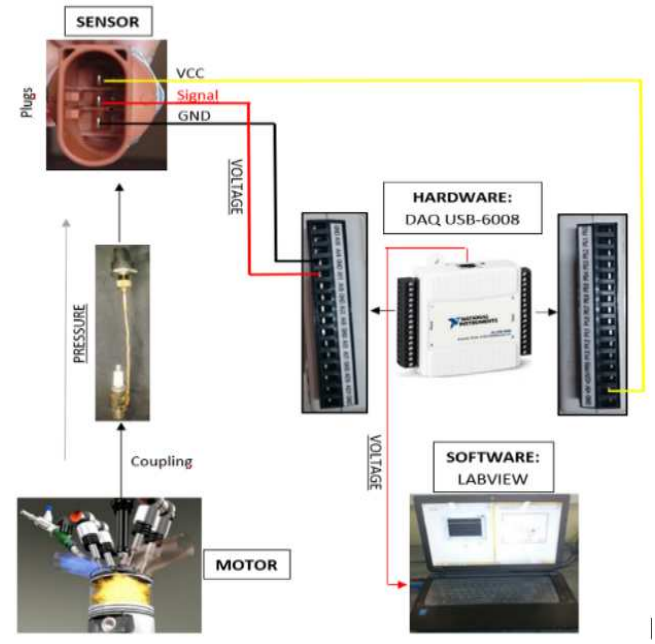

Fig. 13 Schematic diagram of the test system, 1-Acquisition card, 2-Computer, 3-ECU, 4 accelerator position sensor, 5 piezoelectric glass sensor

III. Results and Discussion

A. Signal processing

To obtain the pressure (physical magnitude), the model of Rojas *et al*. [33] measured by the piezoelectric sensor inside the cylinder is used. Creating a function where the pressure depends on the voltage (electrical magnitude) is necessary. For this purpose, in the first instance, the sensor was placed in a Common Rail Direct Injection (CRDi) tester, which can constantly vary and fix the pressure on the fuel rail so that several pressure samples can be taken with the respective voltage provided by the sensor. In addition, the sensor was then coupled together with a pressure gauge on an engine cylinder to sample low pressures with their respective voltages.

The samples are entered in the form of vectors and are rated by the MATLAB, obtaining a grade 2 polynomial shown in eq. (6) governs the sensor's pressure according to its voltage. The mathematical algorithm for signal processing is designed in LabVIEW software with this information.

$$P_R = 1{,}682x^2 + 35{,}45x - 15{,}46 \quad (6)$$

Voltage data and pressure conversion have been used to generate a mathematical model, both magnitudes provided by the built-in pressure sensor. No filter has been implemented as it is necessary to consider the exact and actual behavior of the monitored signal under the different operating conditions of the engine to include and not discard voltage values that may cause the inaccuracy of the developed model. The pressure inside the cylinder without a filter as shown in Figure 14.

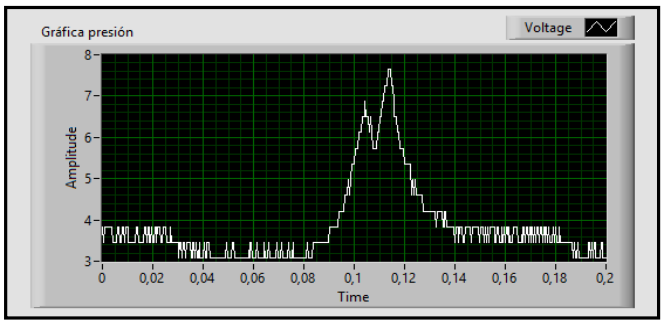

Fig. 14 Pressure without filter obtained in LabVIEW software, an engine without load

B. Development of the Algorithm for the Calculation of Torque and Power

In this section, a statistical analysis of the physical variables extracted from the dynamic tests of the three vehicles cited is carried out in Minitab software, considering that, of the 2500 voltages provided per test performed, the set of samples is further divided into 500 voltages for each analysis; That is, instead of having 17 tests with 2500 voltages for each, 85 tests with 500 voltages are analyzed. This is to generate a more accurate mathematical algorithm based on statistical analysis with a greater number of samples. In order to measure the torque and power of the motorcycle, a model validation process described below was generated concerning the alternative model [33]; otherwise, the bench measurements will be carried out.

C. Torque Calculation

The equipment is connected to capture the data and calculate the torque and power values to generate the resolution comparison based on the catchment parameters, using the alternative torque and power calculation model [1] in addition to the signal strength (equivalent to M.E.P.) that is calculated with Eq. (4) in MATLAB software and engine liter displacement. It should be noted that the tractor force of the tire was also analyzed. However, it did not show a torque-consistent influence. Multiple regression is performed with the three variables cited that affirm the direct influence with torque, as shown in Figure 15. This analysis shows the Eq. (7) governs the torque of vehicles covered by a displacement of different liters.

$$T = -45{,}44 + 1{,}151x_2 - 0{,}796x_3 + 60{,}83x_4 - 0{,}006785(x_2)^2 + 0{,}01139(x_3)^2 + 0{,}1318(x_2) * (x_4) \quad (7)$$

x_2: Signal power
x_3: Vehicle speed (km/h)
x_4: Vehicle displacement (L)

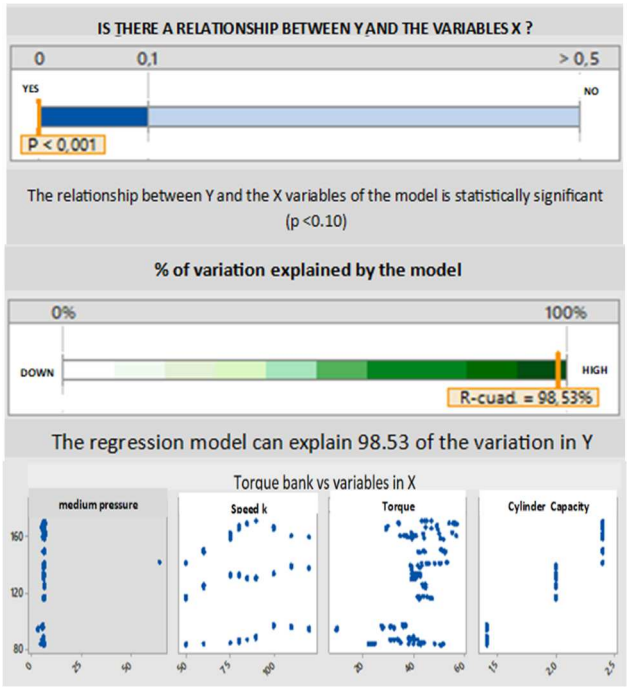

Fig. 15 Multiple regression results for vehicle torque

D. Calculating Power

Similarly, in torque calculation, the results of multiple regression shown in Figure 16 show the direct relationship of engine power to signal strength, vehicle speed, and displacement variables. The statistical analysis is obtained the Eq. (8), which governs vehicles' power within a displacement range of 1.4 to 2.4 liters.

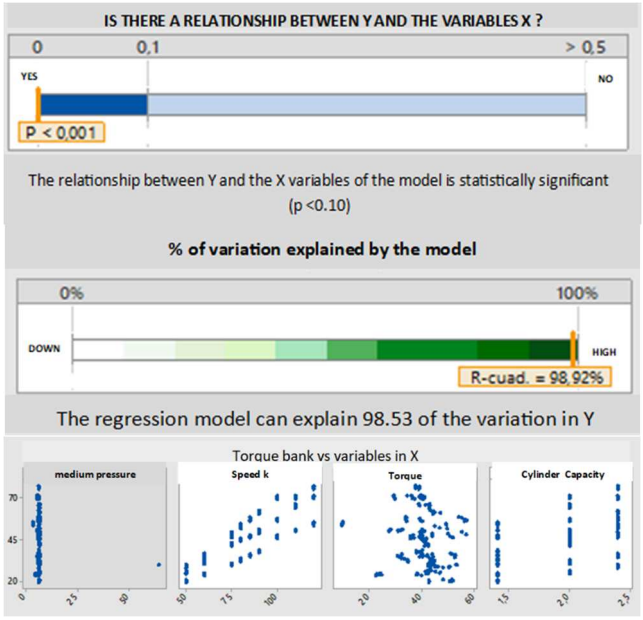

Fig. 16 Multiple regression results for vehicle power

$$P = -20{,}03 + 0{,}2120x_2 - 0{,}714x_3 + 27{,}75x_4 + 0{,}01422(x_3)^2 + 0{,}00587(x_2)^3 + 0{,}0976(x_2) * (x_4) - 0{,}4510(x_3) * (x_4) \quad (8)$$

x_2 : Signal power
x_3 : Vehicle speed (km/h)
x_4 : Vehicle displacement (L)

E. Sensors and Engine Parameters Required for Torque and Power Calculation

Mean Effective Pressure (MEP) comprises the average above atmospheric pressure that gases exert on the plunger during the engine expansion stroke when burned by the action of the electric spark. The M.E.P. is proportional to the torque and for a given rotational speed, also to the supplied power. The calculation of the M.E.P results in determining the pressure inside the cylinder during the engine duty cycle, which is similar to determining the signal strength; For this, a piezoelectric sensor is used that adapts to the spark plug to provide real-time measurements of that internal pressure. In terms of signal processing, signal energy Eq.(10) is a measure that denotes signal strength or size. The energy function of a signal represents the energy dissipated by resistance of 1 ohm when a voltage equivalent to the cylinder pressure signal is applied. Eq. (9) [42] gives the signal energy in the discrete domain.

$$\mathrm{RBW}_{\mathrm{theory}} = \frac{\mathrm{ENBW}}{t_{max} - t_{min}} \quad (9)$$

Where, RBW is the calculation of signal spectra. tmax – tmin, is the duration of the time domain of the selected signal region record duration. ENBW is the equivalent noise bandwidth spectral window. The function estimates signal strength in a single step [43].

$$E = \sum_{n=n_1}^{n_2} |x_n|^2 \quad (10)$$

F. Essential Design Devices

For pressure monitoring purposes inside the cylinder, it is necessary to adapt the spark plug. This involves attaching a metal tube to the spark plug so that the gases are guided from inside the cylinder to the pressure sensor that is adjusted at the end of the cylinder. This is done using a plex and a thin tube. The adaptation made does not impair the correct operation of the cylinder analyzed and the engine in general. The finished coupling is seen in Figure 17 [39].

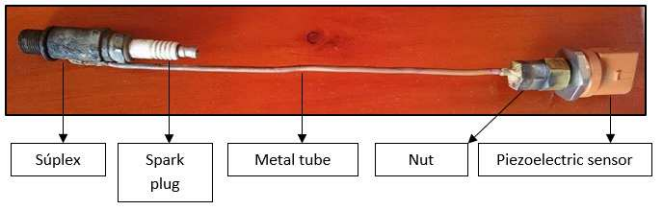

Fig. 17 Spark plug with adapted pressure sensor

G. Engine data collection.

VOLTAGE (V)	PRESSURE (Pa)
0.5	268550
0.51	305698.82
0.53	380097.38
0.52	342881.28

Unchanged original camera

VOLTAGE (V)	SPEED (Km/h)
0.5	0
0.51	20
0.53	40
0.52	60

Unchanged original camera

VOLTAGE (V)	SPEED (Km/h)
0.51	0
0.52	20
0.54	40
0.52	60

Modified camera

VOLTAGE (V)	PRESSURE (Pa)
0.51	305698.82
0.52	342881.28
0.54	417347.12
0.52	342881.28

Modified camera

When measurement of road power with a requirement of 25% as stated in the manufacturer's manual, it can be noted that the results expressed in Table 1 resemble the values obtained, applying the correction by loss of drag which allows us to use the model directly without generating tests on a dynamometric chassis bench. The comparison and analysis of data are carried out, based on the analysis of the curved values obtained in the process of capturing the data by applying the equations described above for the development of the article or research, for which the results are presented in Figure 18 the tractor force generated, in Figure 19 the result of the measured torque and in Figure 20 the final power obtained.

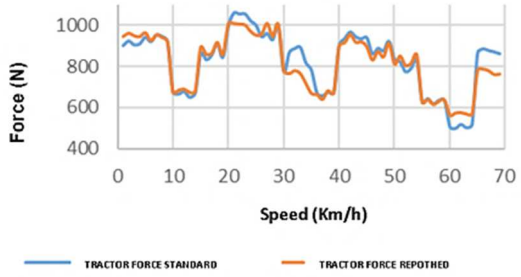

Fig. 18 Tractor force curve behavior graph.

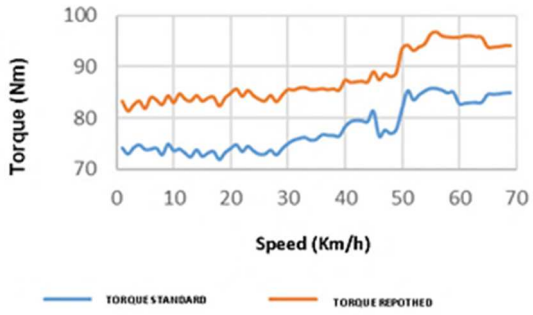

Fig. 19 Torque curve behavior plot.

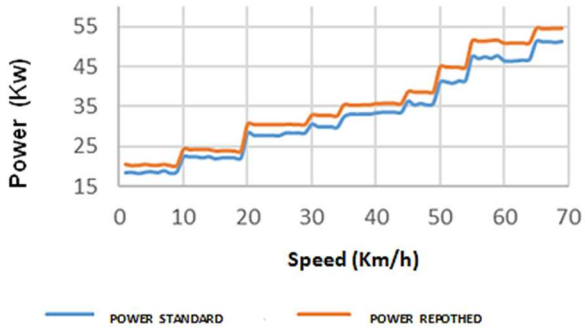

Fig. 20 Graph power curve behavior

IV. Conclusion

Variables such as signal strength, engine displacement, and speed have been used to calculate power and torque, with the signal power directly relating to the values obtained from the pressure calculated by the piezoelectric sensor being a transcendental variable. The configuration inside the data acquisition card is important to capture the signals generated by the engine operation, considering that the rotation revolutions are at high speeds and achieve around 2500 voltage values in a second. This allows achieving exact values over the average pressure in all engine cycles. Emissions were analyzed by observing minor CO, CO2, O2, and HC gases changes. The carburetor feed system possessing that engine does not meet the parameters permitted in the test method determined by the INEN standard for approval of this test.

By modifying the geometry of the combustion chamber, the power was increased by 5.85 kW and the torque 0.78 Nm, verifying an improvement in the increase in combustion characteristics by varying the geometric parameters and the mixing dosing to decrease emissions, with these results getting an improvement of 36.7% and average in the desired parameters. It is important for a model established as a prediction by applying a piezoelectric sensor. The performance in the prediction of the pressure signal is according to the working performance inside the cylinder, and the generated iterations are according to the expected real pressure.

Acknowledgment

The authors are grateful to the Escuela Politécnica Nacional, Universidad Politécnica Salesiana and Escuela Superior Politécnica de Chimborazo for supporting this research.

References

[1] D. Akal, S. Öztuna, and M. K. Büyükakın, "A review of hydrogen usage in internal combustion engines (gasoline-Lpg-diesel) from combustion performance aspect," *Int. J. Hydrogen Energy*, vol. 45, no. 60, pp. 35257–35268, Dec. 2020, doi: 10.1016/j.ijhydene.2020.02.001.

[2] R. Sener, M. U. Yangaz, and M. Z. Gul, "Effects of injection strategy and combustion chamber modification on a single-cylinder diesel engine," *Fuel*, vol. 266, p. 117122, Apr. 2020, doi: 10.1016/j.fuel.2020.117122.

[3] N. X. Khoa and O. Lim, "The effects of combustion duration on residual gas, effective release energy, engine power and engine emissions characteristics of the motorcycle engine," *Appl. Energy*, vol. 248, pp. 54–63, Aug. 2019, doi: 10.1016/j.apenergy.2019.04.075.

[4] B. Amaziane, M. Jurak, L. Pankratov, and A. Piatnitski, "An existence result for nonisothermal immiscible incompressible 2-phase flow in heterogeneous porous media," *Math. Methods Appl. Sci.*, vol. 40, no.

18, pp. 7510–7539, Dec. 2017, doi: 10.1002/MMA.4544.
[5] F. Payri and J. M. Desantes, *Motores de combustión interna alternativos*. Barcelona: Editorial Universitat Politècnica de Valencia, 2011.
[6] M. García López, P. Ponce, L. A. Soriano, A. Molina, and J. J. Rodriguez, "Mejora de la vida útil en los Módulos de Electrónica de Potencia de un BLDCM mediante la Optimización de un Control Difuso," *Rev. Iberoam. automática e informática Ind. (RIAI), ISSN-e 1697-7912, Vol. 16, Nº. 1, 2019, págs. 66-78*, vol. 16, no. 1, pp. 66–78, 2019, Accessed: May 08, 2021. [Online]. Available: https://dialnet.unirioja.es/servlet/articulo?codigo=6723877&info=resumen&idioma=ENG.
[7] P. Leon and C. Piña, "Predicción de emisiones contaminantes de gases de escape a través de la presión media efectiva empleando redes neuronales en motores de encendido provocado," Universidad Politécnica Salesiana, 2018.
[8] T. P. Barbosa, J. J. Eckert, V. R. Roso, F. J. P. Pujatti, L. A. R. da Silva, and J. C. Horta Gutiérrez, "Fuel saving and lower pollutants emissions using an ethanol-fueled engine in a hydraulic hybrid passengers vehicle," *Energy*, vol. 235, Nov. 2021, doi: 10.1016/J.ENERGY.2021.121361.
[9] J. J. Eckert, L. C. D. A. Silva, F. G. Dedini, and F. C. Correa, "Electric Vehicle Powertrain and Fuzzy Control Multi-Objective Optimization, Considering Dual Hybrid Energy Storage Systems," *IEEE Trans. Veh. Technol.*, vol. 69, no. 4, pp. 3773–3782, Apr. 2020, doi: 10.1109/TVT.2020.2973601.
[10] J. Castresana, G. Gabiña, L. Martin, and Z. Uriondo, "Comparative performance and emissions assessments of a single-cylinder diesel engine using artificial neural network and thermodynamic simulation," *Appl. Therm. Eng.*, vol. 185, p. 116343, Feb. 2021, doi: 10.1016/j.applthermaleng.2020.116343.
[11] J. J. Eckert, F. M. Santiciolli, R. Y. Yamashita, F. C. Corrêa, L. C. A. Silva, and F. G. Dedini, "Fuzzy gear shifting control optimisation to improve vehicle performance, fuel consumption and engine emissions," *IET Control Theory Appl.*, vol. 13, no. 16, pp. 2658–2669, Nov. 2019, doi: 10.1049/IET-CTA.2018.6272.
[12] C. Fang, X. Meng, Y. Xie, C. Wen, and R. Liu, "An improved technique for measuring piston-assembly friction and comparative analysis with numerical simulations: Under motored condition," *Mech. Syst. Signal Process.*, vol. 115, pp. 657–676, Jan. 2019, doi: 10.1016/j.ymssp.2018.06.015.
[13] A. García, J. Monsalve-Serrano, S. Martínez-Boggio, V. Rückert Roso, and N. Duarte Souza Alvarenga Santos, "Potential of bio-ethanol in different advanced combustion modes for hybrid passenger vehicles," *Renew. Energy*, vol. 150, pp. 58–77, May 2020, doi: 10.1016/J.RENENE.2019.12.102.
[14] N. D. S. A. Santos, C. E. C. Alvarez, V. R. Roso, J. G. C. Baeta, and R. M. Valle, "Lambda load control in spark ignition engines, a new application of prechamber ignition systems," *Energy Convers. Manag.*, vol. 236, May 2021, doi: 10.1016/J.ENCONMAN.2021.114018.
[15] C. Wen *et al.*, "Online measurement of piston-assembly friction with wireless IMEP method under fired conditions and comparison with numerical analysis," *Meas. J. Int. Meas. Confed.*, vol. 174, p. 109009, Apr. 2021, doi: 10.1016/j.measurement.2021.109009.
[16] M. T. Muslim, H. Selamat, A. J. Alimin, N. Mohd Rohi, and M. F. Hushim, "A review on retrofit fuel injection technology for small carburetted motorcycle engines towards lower fuel consumption and cleaner exhaust emission," *Renewable and Sustainable Energy Reviews*, vol. 35. Elsevier Ltd, pp. 279–284, Jul. 01, 2014, doi: 10.1016/j.rser.2014.04.037.
[17] B. Deng *et al.*, "The challenges and strategies of butanol application in conventional engines: The sensitivity study of ignition and valve timing," *Appl. Energy*, vol. 108, pp. 248–260, Aug. 2013, doi: 10.1016/j.apenergy.2013.03.018.
[18] J. W. Gärtner, Y. Feng, A. Kronenburg, and O. T. Stein, "Numerical investigation of spray collapse in GDI with OpenFOAM," *Fluids*, vol. 6, no. 3, Mar. 2021, doi: 10.3390/FLUIDS6030104.
[19] R. F. Sawyer, "Reformulated gasoline for automotive emissions reduction," *Symposium (International) on Combustion*, vol. 24, no. 1. Elsevier, pp. 1423–1432, Jan. 01, 1992, doi: 10.1016/S0082-0784(06)80166-9.
[20] J. Williams *et al.*, "Effect of Octane Number on the Performance of Euro 5 and Euro 6 Gasoline Passenger Cars," *SAE Tech. Pap.*, vol. 2017-March, no. March, Mar. 2017, doi: 10.4271/2017-01-0811.
[21] Z. Gao *et al.*, "Deep-learning based in-cylinder pressure modeling and resolution of ion current signals," *Fuel*, vol. 282, p. 118722, Dec. 2020, doi: 10.1016/j.fuel.2020.118722.
[22] N. Duarte Souza Alvarenga Santos, V. Rückert Roso, A. C. Teixeira Malaquias, and J. G. Coelho Baêta, "Internal combustion engines and biofuels: Examining why this robust combination should not be ignored for future sustainable transportation," *Renew. Sustain. Energy Rev.*, vol. 148, Sep. 2021, doi: 10.1016/J.RSER.2021.111292.
[23] S. F. da Silva, J. J. Eckert, F. L. Silva, L. C. A. Silva, and F. G. Dedini, "Multi-objective optimization design and control of plug-in hybrid electric vehicle powertrain for minimization of energy consumption, exhaust emissions and battery degradation," *Energy Convers. Manag.*, vol. 234, Apr. 2021, doi: 10.1016/J.ENCONMAN.2021.113909.
[24] A. Joshi, "Review of Vehicle Engine Efficiency and Emissions," *SAE Tech. Pap.*, vol. 2020-April, no. April, Apr. 2020, doi: 10.4271/2020-01-0352.
[25] Z. Guo *et al.*, "Experimental study on combustion and emissions of an SI engine with gasoline port injection and acetone-butanol-ethanol (ABE) direct injection," *Fuel*, vol. 284, p. 119037, Jan. 2021, doi: 10.1016/j.fuel.2020.119037.
[26] B. Yan, H. Wang, Z. Zheng, Y. Qin, and M. Yao, "The effect of combustion chamber geometry on in-cylinder flow and combustion process in a stoichiometric operation natural gas engine with EGR," *Appl. Therm. Eng.*, vol. 129, pp. 199–211, Jan. 2018, doi: 10.1016/j.applthermaleng.2017.09.067.
[27] J. P. Szybist *et al.*, "What fuel properties enable higher thermal efficiency in spark-ignited engines?," *Prog. Energy Combust. Sci.*, vol. 82, Jan. 2021, doi: 10.1016/J.PECS.2020.100876.
[28] M. Alrbai, M. Robinson, and N. Clark, "Multi Cycle Modeling, Simulating and Controlling of a Free Piston Engine with Electrical Generator under HCCI Combustion Conditions," *Combust. Sci. Technol.*, vol. 192, no. 10, pp. 1825–1849, Oct. 2020, doi: 10.1080/00102202.2019.1627340.
[29] B. Işcan, "ANN modeling for justification of thermodynamic analysis of experimental applications on combustion parameters of a diesel engine using diesel and safflower biodiesel fuels," *Fuel*, vol. 279, p. 118391, Nov. 2020, doi: 10.1016/j.fuel.2020.118391.
[30] R. Di Leo, "Methodologies for air-fuel ratio and trapped mass estimation in diesel engines using the in-cylinder pressure measurement," in *Energy Procedia*, Dec. 2015, vol. 82, pp. 957–964, doi: 10.1016/j.egypro.2015.11.850.
[31] V. Rojas, V. Romero, J. Pancha, and J. Martínez, "Analysis of modifications of an internal gasoline combustion engine and determination of torque and power curves applying a mathematical model.," *Rev. Energía y Mecánica Innovación y Futur.*, vol. 1, no. 7, pp. 85–93, 2018, Accessed: May 08, 2021. [Online]. Available: http://repositorio.espe.edu.ec/jspui/handle/21000/18765.
[32] Z. Zhou *et al.*, "Mapping K factor variations and its causes in a modern, spark-ignition engine," *Fuel*, vol. 290, Apr. 2021, doi: 10.1016/J.FUEL.2020.120012.
[33] J. Castillo, V. Rojas, and J. Martínez, "Determination of Torque and Power of a Gasoline Internal Combustion Engine by Using Spark with Pressure Sensor Adapted and Application of a Mathematical Model," *Rev. Politécnica*, vol. 39, no. 1, pp. 49–57, 2017, Accessed: May 08, 2021. [Online]. Available: http://scielo.senescyt.gob.ec/scielo.php?script=sci_abstract&pid=S1390-01292017000100049&lng=en&nrm=iso.
[34] M. Tadros, M. Ventura, and C. G. Soares, "Data driven in-cylinder pressure diagram based optimization procedure," *J. Mar. Sci. Eng.*, vol. 8, no. 4, Apr. 2020, doi: 10.3390/JMSE8040294.
[35] T. Skrzek *et al.*, "Repeatability of high-pressure measurement in a diesel engine test bed," *Sensors (Switzerland)*, vol. 20, no. 12, pp. 1–12, Jun. 2020, doi: 10.3390/s20123478.
[36] D. Stannard, D. Quinn, C. Hill, and C. Johansen, "Experimental investigation of self-pressurized propellant injection into a simulated rocket motor combustion chamber," *Int. J. Multiph. Flow*, vol. 142, Sep. 2021, doi: 10.1016/J.IJMULTIPHASEFLOW.2021.103707.
[37] H. G. Zhang, X. J. Han, B. F. Yao, and G. X. Li, "Study on the effect of engine operation parameters on cyclic combustion variations and correlation coefficient between the pressure-related parameters of a CNG engine," *Appl. Energy*, vol. 104, pp. 992–1002, Apr. 2013, doi: 10.1016/j.apenergy.2012.11.043.
[38] B. L. Salvi and K. A. Subramanian, "Experimental investigation and phenomenological model development of flame kernel growth rate in a gasoline fuelled spark ignition engine," *Appl. Energy*, vol. 139, pp. 93–103, Feb. 2015, doi: 10.1016/j.apenergy.2014.11.012.
[39] J. Toala and D. Vistín, "Estudio experimental para determinar los parámetros de torque, potencia, consumo y emisiones de un motor de cuatro tiempos, monocilíndrico de 200cc, al variar la geometría de la cámara de combustión.," 2019.

[40] G. Genta and L. Morello, “Prime Movers For Motor Vehicles,” in *The Automotive Chassis*, Springer Netherlands, 2009, pp. 165–184.
[41] C. P. O. Treutler, “Magnetic sensors for automotive applications,” *Sensors Actuators, A Phys.*, vol. 91, no. 1–2, pp. 2–6, Jun. 2001, doi: 10.1016/S0924-4247(01)00621-5.
[42] J. M. Riesco-Ávila, A. Gallegos-Muñoz, J. M. Montefort-Sánchez, and S. Martínez-Martínez, “Alternative Combustion Processes in Internal Combustion Engines,” *Acta Univ.*, vol. 15, no. 1, pp. 36–54, Apr. 2005, doi: 10.15174/au.2005.227.
[43] The MathWorks Inc., “Medir el poder de una señal - MATLAB & Simulink - MathWorks América Latina.” https://la.mathworks.com/help/signal/ug/measure-the-power-of-a-signal.html (accessed May 08, 2021).